FORSCHUNGSZENTRUM ROSSENDORF
Mitglied der Wissenschaftsgemeinschaft Gottfried Wilhelm Leibniz

WISSENSCHAFTLICH-TECHNISCHE BERICHTE
FZR-385
Juli 2003
ISSN 1437-322X

Jan Džugan

Crack lengths calculation by the unloading compliance technique for Charpy size specimens

Herausgeber:
Forschungszentrum Rossendorf e.V.
Postfach 51 01 19
D-01314 Dresden
Telefon +49 351 26 00
Telefax +49 351 2 69 04 61
http://www.fz-rossendorf.de/

Als Manuskript gedruckt

FORSCHUNGSZENTRUM ROSSENDORF
WISSENSCHAFTLICH-TECHNISCHE BERICHTE
FZR-385
Juli 2003

Jan Džugan

Crack lengths calculation by the unloading compliance technique for Charpy size specimens

Contents:

Abstract

The problems with the crack length determination by the unloading compliance method are well known for Charpy size specimens. The final crack lengths calculated for bent specimens do not fulfil ASTM 1820 accuracy requirements. Therefore some investigations have been performed to resolve this problem. In those studies it was considered that the measured compliance should be corrected for various factors, but satisfying results were not obtained. In the presented work the problem was attacked from the other side, the measured specimen compliance was taken as a correct value and what had to be adjusted was the calculation procedure. On the basis of experimentally obtained compliances of bent specimens and optically measured crack lengths the investigation was carried out. Finally, a calculation procedure enabling accurate crack length calculation up to 5mm of plastic deflection was developed. Applying the new procedure, out of investigated 238 measured crack lengths, more than 80% of the values fulfilled the ASTM 1820 accuracy requirements, while presently used procedure provided only about 30% of valid results. The newly proposed procedure can be also prospectively used in modified form for specimens of a size different than Charpy size.

1 Introduction

The traditional multiple specimen method for fracture toughness measurement is highly material and time consuming. To reduce this effort, single specimen methods were developed. One of the most used single specimen method is the unloading compliance method (UC), which is also included into ASTM and ISO standards [1, 2]. The UC method provides sufficient results for CT specimens, but in the case of three-point bend specimens problems were encountered, especially for small Charpy size specimens, limiting the use of this method. In order to overcome this drawback, an investigation was carried out to improve the UC methodology and to provide reliable results for the considered specimen geometry.

The problem of the crack length determination using UC is already well known and several investigations [3-7] have been carried out to solve this problem, but no satisfactory solution has been found. The problem is that as soon as the specimen is bent, the standard formulas for the crack determination provide shorter crack lengths than optically measured. The accuracy limits discard the specimens with larger deviation of the calculated crack lengths from the measured values and so these specimens should not be included in the evaluation. The error is increasing with increasing deflection. The materials with low resistance against the crack growth can be tested and the standards limits can usually be fulfilled, but in case of the materials with high resistance against the crack growth, as reactor pressure vessel steels, large deflections have to be reached before stable crack growth starts but the inaccurate results of the crack extension measurement make these results invalid.

For solving this problem, literature survey was performed and subsequently available experimental data were summarized as the base for solution. Additionally, some further tests were also carried out. In this way enough data were available to derive a correction procedure.

To obtain reference values, initial and final crack lengths were optically measured on each specimen as well.

2 Description of the UC method

The method is based on the change of the body stiffness or compliance, with advancing crack size. In the case of the fracture toughness specimens is usually measured crack mouth opening compliance with the use of a suitable gauge. From the measured specimen compliance C, and the specimen geometry given by the thickness B, the width W, the crack length a and the span S, the elastic modulus E and a suitable calibration function the actual crack length can be obtained. The elastic modulus and geometry of the specimen are known, so the only "unknown" is the calibration function. This function is in the standards, derived for straight specimens.

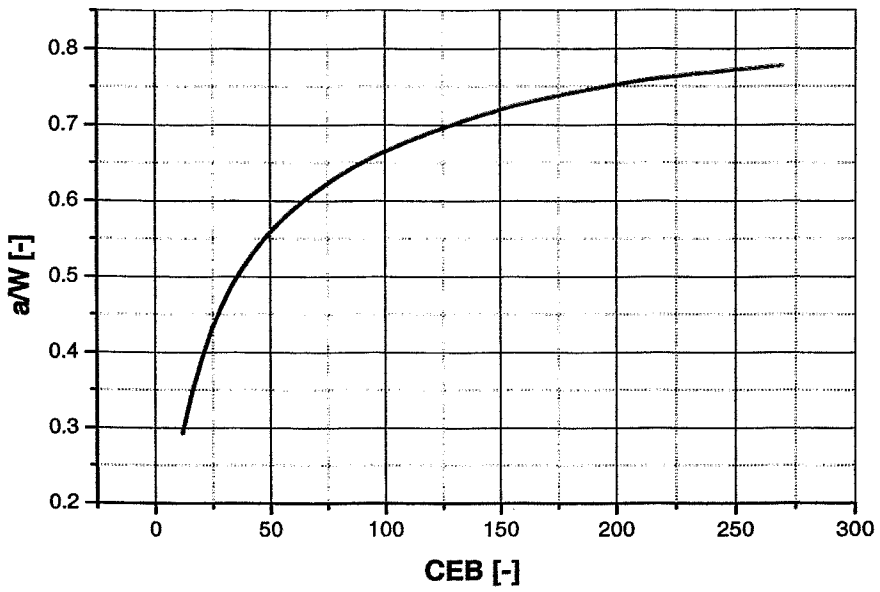

Fig. 1. a/W versus normalized compliance (CEB) plot

The shape function is derived from the relation of two normalized values a/W and CEB, so simple transferability from specimen to specimen should be assured. The graph of the dependence of a/W on CEB is shown in Fig. 1. This function can be easily transformed into simpler function by introducing the parameter μ according to Eq. 1. When this parameter is used the trend demonstrated in Fig. 2 is obtained. This transformed relation is further used for the determination of the shape function. In the standard the polynomial of the fifth degree is fitted to this curve. The shape function in this form can be easily obtained if set of several specimens with known crack lengths covering the range of interest, for Charpy specimens it is approximately from 4mm to 7mm, are tested. The specimens are elastically loaded, the compliance is measured and the shape function can be plotted.

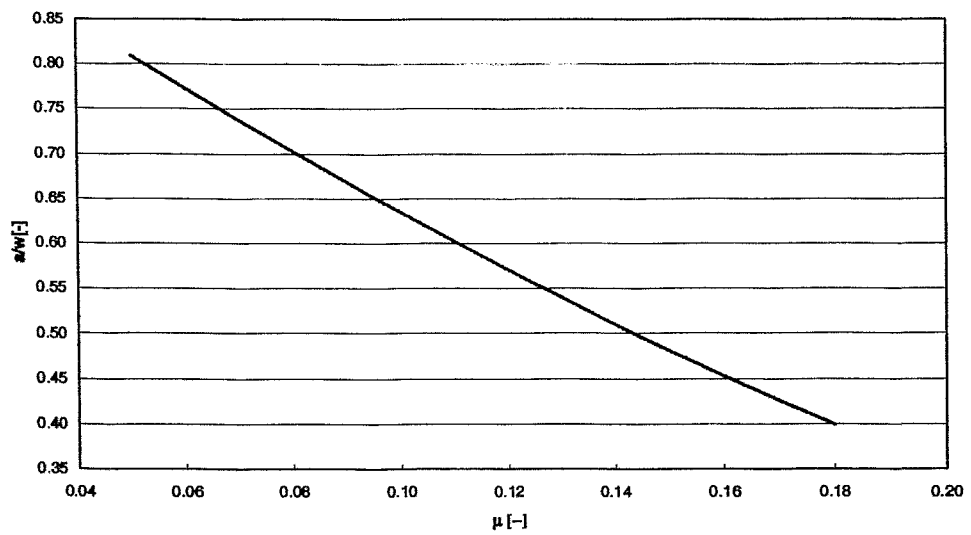

Fig. 2. Calibration curve for three point bend specimens

The crack length ***a*** can be calculated from following equation, Eqs. 2, according to [1,2]:

$$\mu = \frac{1}{1 + \sqrt{B_e \bullet E \bullet C \bullet \frac{W}{\frac{S}{4}}}} \tag{1}$$

$$a = W \bullet \left(0.999748 - 3.9504 \bullet \mu + 2.9821 \bullet \mu^2 - 3.21408 \bullet \mu^3 + 51.51564 \bullet \mu^4 - 113.031 \bullet \mu^5\right) \tag{2}$$

$$B_e = B - \frac{(B - B_N)^2}{B} \tag{3}$$

where :

S	span	[mm]
B	specimen thickness	[mm]
B_N	specimen net thickness	[mm]
W	specimen width	[mm]
C	specimen compliance	[mm/N]
E	elastic modulus	[GPa]

3 UC correction techniques proposed

Generally, the unloading compliance based crack lengths are under-predicted for deformed three point bent specimens. There are more ways how can be this problem treated. Probably the easiest one is division of the calculated final crack extension by measured final extension. All calculated crack extension could be subsequently multiplied by this ratio and J-integral determined with the corrected crack growth values. With this method always valid values can be obtained, but there is no real background for the use of such a method.

The other way in which could be attacked the problem is detailed analyse of the test. The most detailed investigation on the effects taking place during the bending of the specimen on the compliance measurement was performed by Steenkamp [3, 4]. Further work in this field was done by Ipiña [5] who partly used Steenkamp's results and tried to find out additional the geometrical impacts due to the specimen bending. In a previous work Džugan [6,7] also tried to resolve this problem by means of the empirically determined compliance change in dependence on deflection.

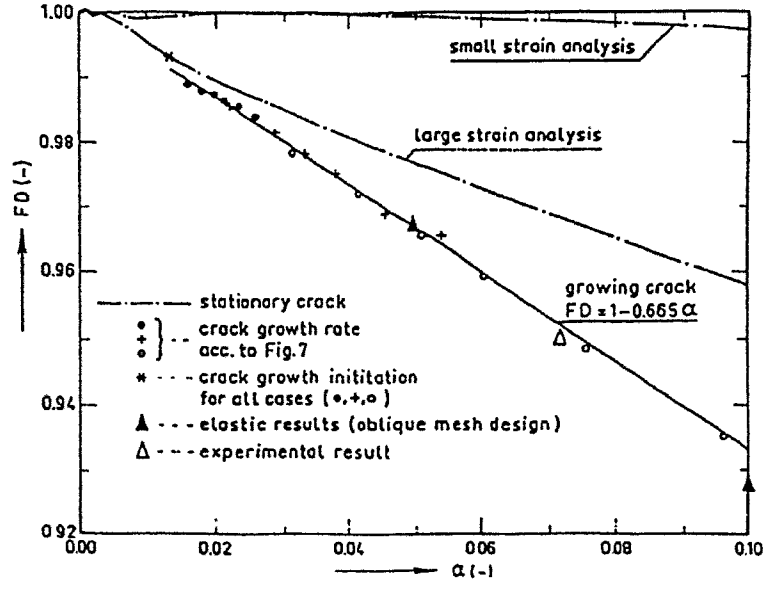

Fig. 3 Deformation correction coefficient [3]

Steenkamp performed his investigation on three-point bend specimen with the cross section 12.5mm x 25 mm. He investigated the effects of the striker indentation FI, the specimen deflection FD, the change of the span caused by a test-piece bending FR and finally crack front curvature FC. He tried to quantify all of those effects and summarized their effect on the UC evaluation in corrected value of compliance C_e, Eq. 4.

$$C_e = \frac{C}{\frac{FC}{FC_0} \bullet \frac{FD}{FD_0} \bullet \frac{FR}{FR_0} \bullet \frac{FI}{FI_0}} \tag{4}$$

Crack front curvature correction factor (FC) for test pieces fulfilling ASTM requirements for the crack front curvature attains value less than 1 %. The change of span during the test together with assumed friction between the sample and rollers, FR, affects the compliance by about 1%. The striker indentation into the specimen surface affects the test in terms of slight change of loading conditions from pure 3 point bending. In this case the load is not transmitted by a discrete line, but is distributed over an area. The value of the factor FI is also about 1% as in the previous cases. Finally, the last correction factor FD takes into account the sample deflection. Its value increases with increasing deflection and this factor seems to be predominant, especially at higher deflection values. Dependence of FD on deformation for the specimen with growing crack is shown in Fig. 3. Steenkamp proposed FD in following form [3, 4]:

$$FD = 1 - 0.665 \bullet \alpha \tag{5}$$

$$\alpha = \frac{\Delta}{2 \bullet W}$$

where Δ is load line displacement.

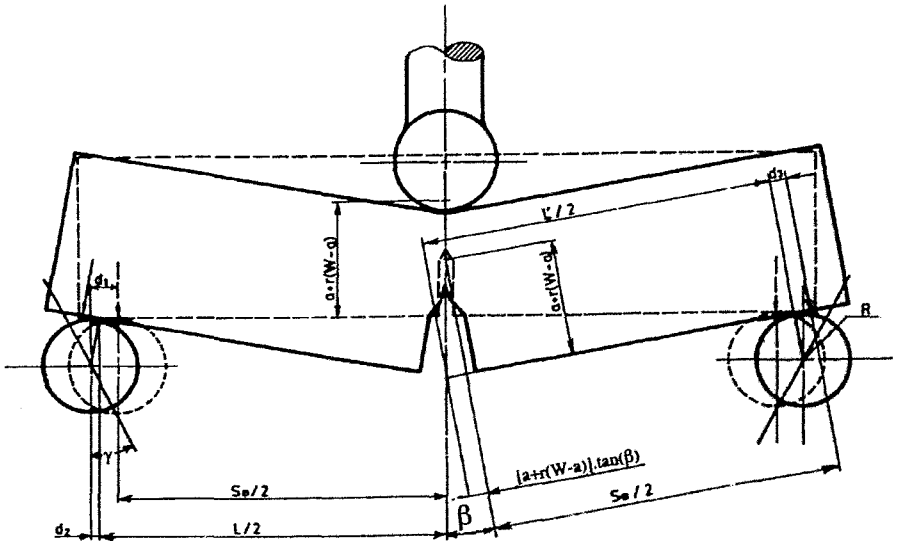

Fig. 4 Three point bend test [5]

Ipiña and Santarelli [5] considered the test kinematics. Three-point bend specimen during the bending is deformed as two rigid arms rotating around the apparent centre of rotation. During this movement the rollers (support pins) move, so the span during the tests is not constant. In order to correct calculated crack lengths, two corrections are applied: displacement correction (DC) and load correction (LC). Displacement correction estimates the error of the crack mouth opening measurement due to the specimen rotation, Eq. 6. The load correction takes into account the change in the span and thus the loading moments are also changed, Eq. 7.

$$DC = \frac{\cos \beta_0}{\cos(\beta + \beta_0)} \tag{6}$$

where : $\beta = a\tan\frac{\Delta}{\frac{S_0}{2}}$ and $\beta_0 = a\tan\left(\frac{D}{2\bullet(a+r\bullet(W-a))}\right)$

a	crack length	[mm]
β_0	initial crack mouth opening angle	[rad]
β	rotation angle	[rad]
D	initial crack mouth opening	[mm]
r	rotation factor; r = 0,45	[-]
S_0	initial span	[mm].

$$FC = \frac{\frac{2}{1+\cos\beta}\bullet(S_0 - R\bullet(\beta+\sin\beta))}{S_0} \tag{7}$$

where R is the roller radius.

Finally, the corrected compliance $C_{c\text{-Ipiña}}$ can be determined according to following relation:

$$C_{c-Ipina} = C_m \bullet \frac{DC}{FC} \tag{8}$$

where C_m is the measured crack mouth opening compliance.

4 Experimental program

In order to check the performance of the published correction functions or to propose a new one, wide range of material behaviour had to be covered and sufficient amount of data had to be available. The materials and experimental costs were reduced by using previously tested specimens used for J-R curves evaluation. Wide range of the specimen deflections as well as the crack extensions were considered. Whenever the number of the tests was insufficient for a considered deflection or crack length level, further tests were carried out.

4.1 Materials

The materials used for the investigation had to provide a wide range of deflection-crack length combinations so that the validity of the correction procedure could be tested for a wide range of applications. The available data collection fulfilled this. Here the strength-toughness behaviour of the low alloy heat resistant 10CrMo9-10 steel was varied by 5 different heat treatments. Additionally, the medium carbon steel SFA was involved. Chemical compositions, heat treatments and mechanical properties of the investigated materials are given in Tabs. 1-3.

Tab 1. Chemical compositions of the investigated materials

Material	Weight %								
	C	Si	P	S	Mn	Cr	Ni	Cu	Mo
10 CrMo 9 10	0.14	0.32	0.007	0.021	0.504	2.31	0.106	0.155	0.99
SFA	0.38	0.26	0.010	0.006	0.78	---------	---------	---------	---------

Tab 2. Heat treatments of 10 CrMo9-10 steel

Designation	Heat treatment
C	950°C / oil + 640°C / 2h
D	950°C / 1h / oil + 600°C / 2h
E	950°C / 1h / oil + 640°C / 2h
F	950°C / 1h / oil + 720°C / 2h
G	950°C / 1h / oil + 760°C / 2h

Tab 3. Mechanical properties of the investigated materials

Material	E [GPa]	$R_{p0.2}$ [MPa]	R_m [MPa]	A [%]	Z [%]
10 CrMo 9 10 - C	210	697*	1006*	---	---
10 CrMo 9 10 - D	206	742	846	15.9	73
10 CrMo 9 10 - E	207	634	728	18,6	79,0
10 CrMo 9 10 - F	201	446	565	27,7	80,1
10 CrMo 9 10 - G	198	389	511	35,6	80,7
SFA	204	363	608	32	---

*data evaluated from three point bend specimens

4.2 Testing

The batch of investigated materials consisted of two groups of specimens. The first group were the specimens previously tested. These specimens were tested in accordance with ASTM 813 or later ASTM1820 and J-R curves were evaluated.

The second group of the specimens were the specimens specially tested for this study and thus some special procedures were applied. Some of the specimens were tested so that several steps of crack progress can be optically measured on one specimen. The procedure consists of monotonic loading up to desired deflection levels, followed by fatigue crack extension and further monotonic loading. Before each of monotonic loadings or fatigue crack extensions, the elastic compliance of the specimen was measured. This procedure provided specimens with up to 12 different crack lengths. An example of the fracture face of the specimen tested according to described procedure can be seen in Fig.5.

The second special procedure of the specimen preparation and testing was the procedure providing desired crack lengths at pre-selected deflections. The purpose of these specimens was to provide data for calibration curves determination at several deflection levels. Three sets of specimens were prepared for following deflections: 1, 2 and 3 mm. Each set consisted of six specimens with crack lengths ranging from 4.5 up to 7mm. In this case V-notched specimens were firstly bent up to desired plastic deflection and subsequently the notches were extended by electro-erosive-discharging providing a straight crack of known length, Fig. 6. In order to make sure that this procedure provides comparable data with usually tested specimens, the compliances at similar deflections and crack lengths for the specimens tested according to standard and our method were compared. The comparison showed that data belong to the same population and thus can be further used for the investigation together with the other collected data.

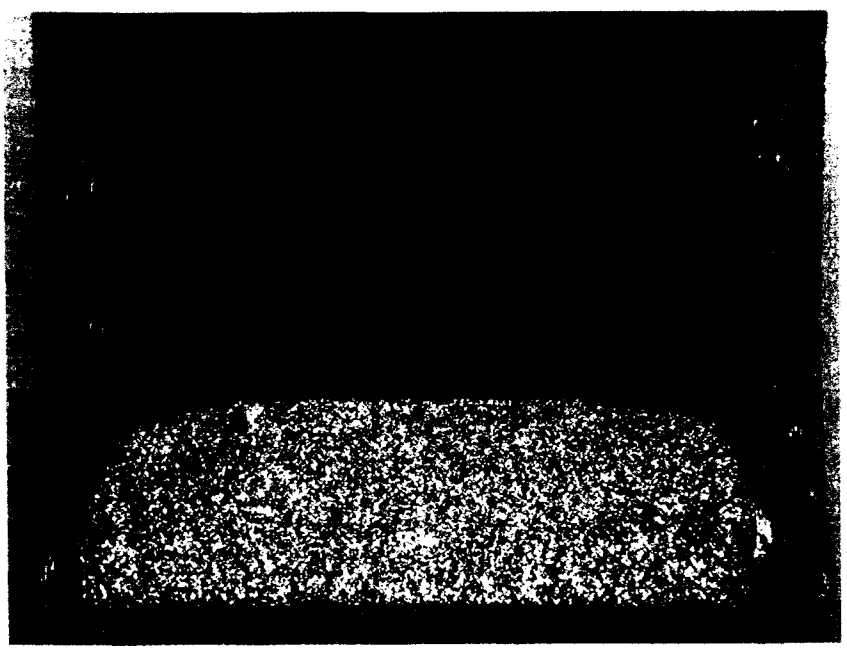

Fig. 5. Multiple-cracked specimen

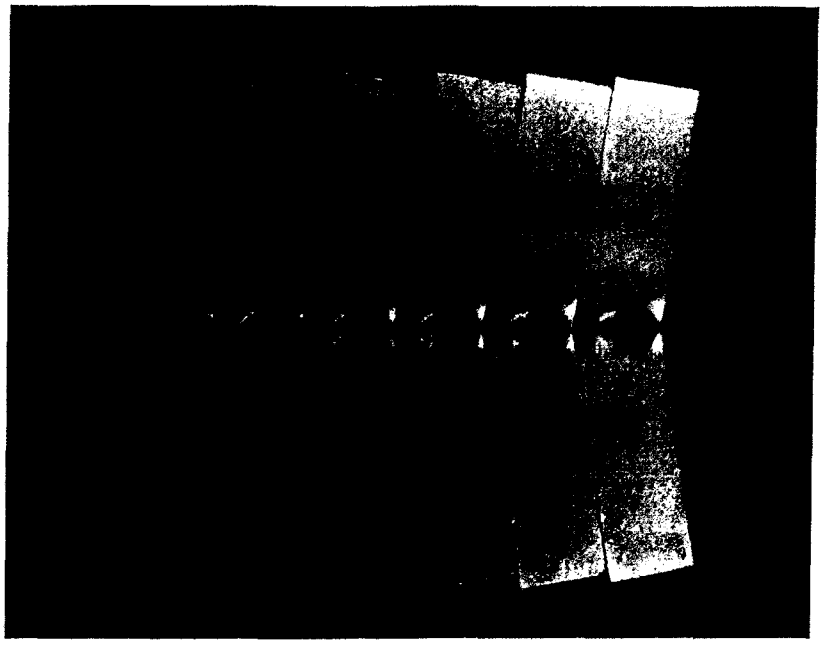

Fig. 6. Set of bent and notched specimens at deflection 3mm

All the specimens were side-grooved Charpy specimens, except the bent and eroded specimens for the second procedure. The side-grooved specimens were firstly pre-cracked and then side-grooved.

The use of non-side-grooved bent + eroded specimens was suggested to attain a higher force capacity of the specimens. This was especially important in the case of deeply notched specimens when the forces for the compliance measurement would be on the lower threshold of the testing machine operation range, not assuring sufficient measurement accuracy.

4.3 Crack lengths measurement

Having the problems with the crack lengths determination, both sides should be observed, UC crack length based evaluation and the optical measurement.

According to the standards [1, 2] it is usual to measure the initial and final crack length after the test by means of an optical method and to compare the results with the crack length determined by the UC technique. In general, this is no problem in the case of the initial crack length measurement if the measuring equipment is perfectly working. In case of the final crack length measurement the situation is more complicated and as a results of that, relatively large discrepancies are found. This is not only caused by the geometry of the deformed specimen that changes slightly, but also because the crack is not any more as straight as at the beginning of the test. The specimen compliance provides information about a representative or average crack length of the specimen. In the case of the optical crack length measurement the crack is measured at several equidistantly distributed positions and then the values are averaged. The crack lengths near to surface have to be measured according to ASTM 1820 in distance 0.005·W, which means 0.05mm for Charpy size specimens. This position lays for deformed specimen in many cases in the region of lateral contraction and if the nearest crack extension reaching the specimen side surface is used, very

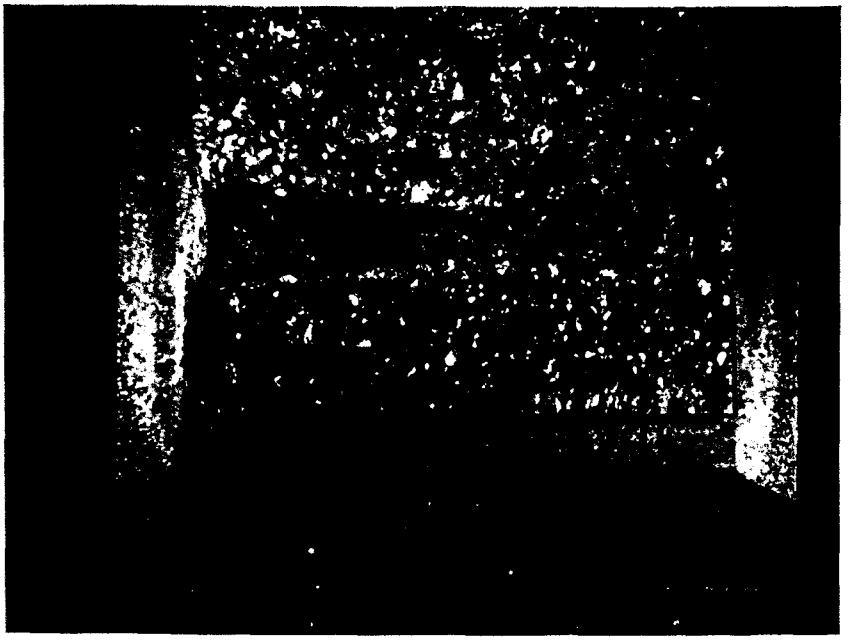

Fig. 7. Crack length measurement – area method - specimen 321

high values of crack extension can be obtained not corresponding with the real crack length. In GKSS procedure [8] it is mentioned that area-averaged method should provide most reliable results, but 9-point average yields acceptable results, which was checked further.

As a check of the crack length measurement accuracy, the crack lengths obtained with various methods were compared. Optical microscope and stereomicroscope with digital camera were used. Optical measurement followed the standardized 9-point procedure, Δa_m. In case of digital pictures of the fracture surfaces two methods were applied. The first was the 9-point method, Δa_{9point} , for the direct comparison with optically measured values. The second one used area-averaged measurement of the cracks, Δa_{area}, Fig. 7. The crack area was measured and the crack length was calculated by dividing the measured area by the specimen thickness. The results of these measurements are summarized in Tab. 4 and compared in Tab. 5.

Tab. 4. Crack lengths measured by different techniques

Specimen	Optical measurement		Digital photo				Unloading Compliance	
			Area method		9 point method			
	a_{om}	Δa_m	a_{oarea}	Δa_{area}	$a_{o9Point}$	Δa_{9point}	a_{0UC}	Δa_{UC}
237	5.03	1.18	5.09	1.11	5.09	1.13	4.96	1.02
238	4.96	1.27	5.02	1.15	5.00	1.26	5.06	0.97
299	4.97	1.28	5.02	1.15	5.02	1.23	4.89	1.08
321	5.02	1.19	5.08	1.01	5.05	1.12	4.95	0.98
322	5.01	1.25	4.98	1.14	4.98	1.24	4.93	1.06
D2-3	4.90	1.65	4.91	1.64	4.92	1.61	4.93	1.48
D2-5	4.93	1.80	4.93	1.79	4.92	1.79	4.96	1.65
E3-137	4.96	1.35	4.96	1.35	4.94	1.38	4.90	1.15
E3-145	4.99	0.96	5.07	0.91	5.05	0.92	4.91	0.83
F2-7	5.06	0.79	5.11	0.75	5.12	0.77	5.06	0.63
F2-8	5.13	0.58	5.19	0.56	5.14	0.62	5.04	0.48

Tab. 5. Comparison of the different crack length measurement techniques

Specimen	Δa_m-Δa_{9point}	Δa_m-Δa_{area}	Δa_m-Δa_{UC}	Δa_{area}-Δa_{UC}	a_{om}-$a_{o9Point}$	a_{om}-a_{oarea}
237	0.05	0.08	0.16	0.08	-0.06	-0.06
238	0.02	0.13	0.30	0.17	-0.05	-0.06
299	0.06	0.14	0.20	0.07	-0.05	-0.05
321	0.07	0.18	0.21	0.03	-0.03	-0.06
322	0.01	0.11	0.19	0.08	0.03	0.03
D2-3	0.03	0.01	0.17	0.16	-0.03	-0.01
D2-5	0.01	0.01	0.15	0.14	0.01	0.00
E3-137	-0.03	-0.01	0.20	0.20	0.02	0.00
E3-145	0.04	0.05	0.13	0.07	-0.06	-0.09
F2-7	0.02	0.04	0.17	0.13	-0.06	-0.05
F2-8	-0.04	0.02	0.10	0.09	-0.01	-0.06
Median	0.02	0.05	0.17	0.09	-0.03	-0.05

The first comparison could be made for the initial crack lengths because the crack front is even and more or less straight. It can be inferred from Tab. 4, that both methods using digital picture provide almost the same values, whereas the optically measured initial crack are slightly shorter. This could point to a systematic error caused by an effect of the different illumination conditions in both microscopes used or, more probably, by an error of the magnification calibration. Magnification setting on the stereomicroscope is not robustly conditioned. In every case, the error is really minimal and thus the data are comparable.

Concerning the final crack extension there is a good agreement between the optically measured values and the values obtained from digital pictures with 9-point method. The area method had also good agreement with optically measured values for a part of the investigated sample, but the specimens with more complex crack shape exhibit a big error. Comparing to the optical 9-point method the cracks are noticeably longer that those calculated from the measured area. The fact gives a hint that for more complex crack shapes the 9-point method over-estimates the crack lengths. This is partly compensated by the straightness criterion in the ASTM standard [1]. It excludes specimens with too strong curvature of the crack front.

Generally, it can be expected longer cracks determined for the specimens with curved crack tip when the 9-point average method is used.

5 Results and evaluation

The collected data file consisted of over 240 calculated and measured crack lengths at various deflections. Data covered the crack lengths range from 3.8 to 8.1 mm and deflections up to 7.2 mm. The accuracy of the calculated and the measured initial crack lengths was observed and in the cases in which the error exceeded 0.1mm the data were excluded from further analysis. In case of smaller errors the effective Young's modulus was determined so that calculated and measured initial crack length values were the same. This calculation was performed to decrease the number of variables and to define some common basis so that the crack extensions could be consistently evaluated and the only error included in the final crack length determination were related to the specimen deformation. Finally, 238 crack lengths were available for a further analysis. The data available were: measured crack length, initial and crack mouth opening compliance, specimen elastic and plastic deflection and specimen dimensions.

Present UC crack calculations are based on the calibration curved derived for a straight specimen. In the first step it was checked if the calibration function for the straight specimen is also valid for the bent one. It was found that the calibration curve for the straight specimen creates a lower bound for the other curves of the deformed specimens. The calibration curves for bent specimens were moving upwards. Obviously the curves move in dependence on the specimen's deflection and so the data were divided into several groups according to the deflection. Because of variable elastic properties of the materials, plastic deflection was considered as a more general

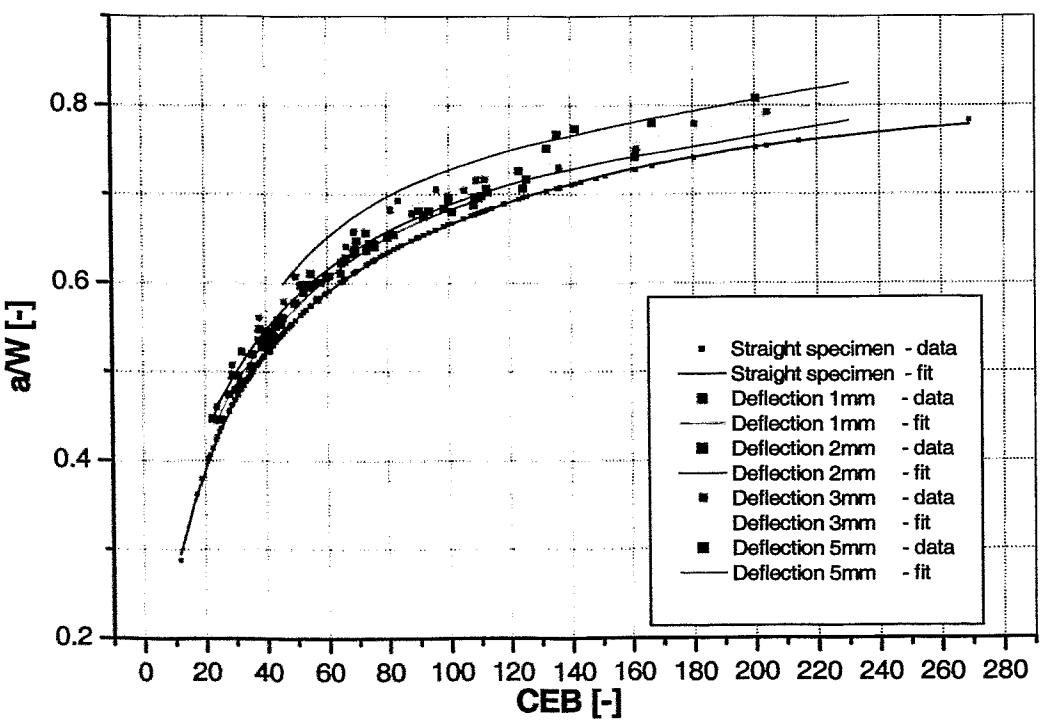

Fig.8. Shift of a/W versus CEB curves in dependence on deflection

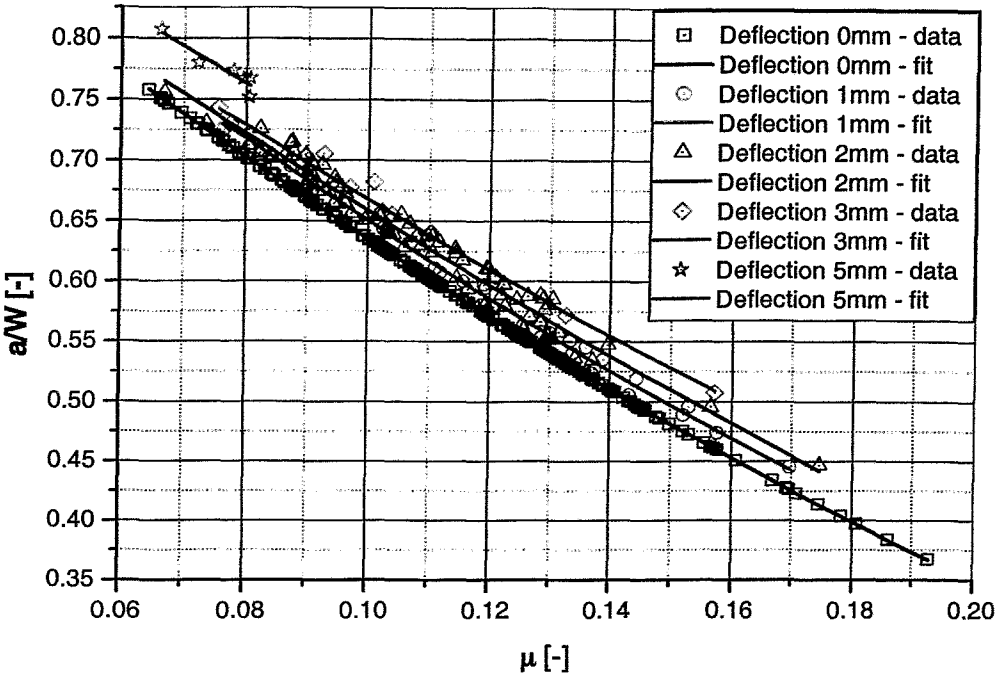

Fig. 9. Shift of the calibration curves with deflection mm

value for the further evaluation. Data were divided into groups of 0.5mm step width. It is almost impossible to find the specimens with exact plastic deflection fitting to desired value and so values ±0.2mm were included into each group. Groups with 0, 0.5, 1, 1.5, 2, 2.5, 3, 3.5 and 5 mm plastic deflections were obtained. When these data are plotted together in dependence on measured crack lengths and normalized compliances, trend depicted in Fig. 8 can be found. There is clearly visible an increasing shift of the curves from the standard one with increasing deflection. If the data are transformed with the use of Eq. 1, relations displayed in Fig. 9. are obtained. The trend of the curves hints that for deflected specimens another calibration functions for the crack determination have to be used than for the straight specimens.

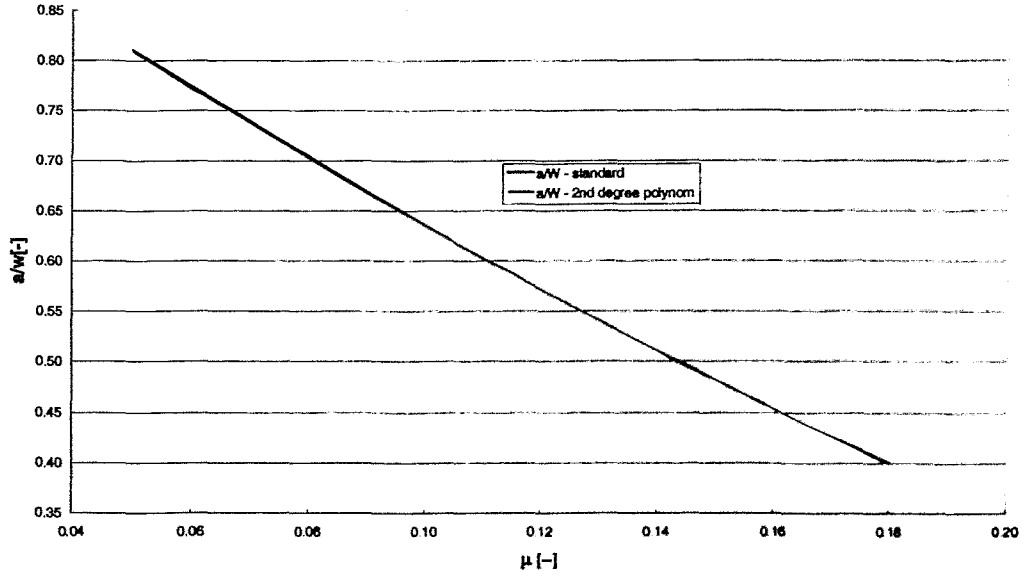

Fig. 10. Comparison of simplified and original calibration curve for straight specimen

Tab. 6. Comparison of Standard calibration function and simplified curve

μ [−]	$a/w_{standard}$ [−]	a/w_{cor} [−]	Error [%]
0.050	0.810	0.808	0.21
0.055	0.791	0.790	0.21
0.060	0.773	0.772	0.20
0.065	0.755	0.754	0.19
0.070	0.738	0.736	0.18
0.075	0.720	0.719	0.17
0.080	0.703	0.702	0.15
0.085	0.686	0.685	0.13
0.090	0.669	0.668	0.10
0.095	0.652	0.651	0.08
0.100	0.635	0.635	0.05
0.105	0.619	0.619	0.03
0.110	0.603	0.603	0.00
0.115	0.587	0.587	-0.02
0.120	0.571	0.571	-0.04
0.125	0.555	0.556	-0.06
0.130	0.540	0.540	-0.08
0.135	0.525	0.525	-0.09
0.140	0.510	0.510	-0.09
0.145	0.495	0.496	-0.08
0.150	0.481	0.481	-0.07
0.155	0.467	0.467	-0.05
0.160	0.453	0.453	-0.01
0.165	0.439	0.439	0.03
0.170	0.426	0.425	0.09
0.175	0.412	0.412	0.16
0.180	0.399	0.398	0.25

The even increase of the curves with increasing deflection encourages description of the calibration curves change by means of the deflection. Now the crucial point is to decide if the curves are moving upwards with increasing deflection or are rotating around some common point. Closer observation of the curves reveals that they are rotating. If the curves are rotating do they have common rotation point? Observing the Eq. 1, it could be concluded that for the specimen with crack through whole specimen width, a/W=1, the specimen stiffness should be 0, the compliance should be theoretically infinite and thus μ=0. This point should be then common for all calibration curves regardless of the specimen deflection. Having found that the calibration curves are rotating around one centre point, subsequent step should be the description of the curves rotation with increasing deformation.

To be able to describe the curves rotation it was firstly decided that as a parameter describing the specimen deformation, plastic angle, α_{pl}, instead of plastic deflection is further used. The reason for this was easier transferability of the calibration curves shift to the other dimensions of the specimens than in the case of total deflection. The second problem was how the rotation could be described. From the practical point of view it would be useful if one equation could take into account all the effects. To be able to realize it some simplifications were used. The first one was the minimization

of the problems with polynomials. Several polynomials were tested, polynomials of 2^{nd}, 3^{rd} and 4^{th} degree, and compared with presently used polynomial of 5^{th} degree. The error of the polynomial of 2^{nd} degree in comparison with standard function was within 0.25% for a/W ratio ranging from 0.4 to 0.81, Tab. 6., Fig 10. All performed tests should fall within this range if initial crack lengths and maximum crack extensions recommendations according to ASTM 1820 are followed. According to the standard the minimal a_0/W can be minimally 0.45 and maximally 0.7. Taking into account maximum crack capacity for a specimen allowed by the standard the maximum value $a_f/W = 0.775$ can be reached. This value is still well within the range with good agreement between standard calibration function and the simplified one, Eq. 9.

$$\frac{a}{W} = A\mu^2 + B\mu + 1 \tag{9}$$

After the shape of a searched function was found, the second step was to get representative data that could be used for the evaluation of the deflection on the calibration curves. In the case of straight specimen, the calibration function can be obtained if elastic compliance of several specimens of known crack lengths is measured. In order to determine the calibration function in the same way, but for bent specimens, specially prepared bent + eroded specimens were provided. Before a bigger batch of such specimens was prepared, two trial specimens were firstly used in order to be certain that the specimens prepared in proposed way represent behaviour of standard specimens. When these two trials specimens were tested they were put together with the data obtained with standard specimens at comparable deflection level. The trial specimens data agreed very well with the other data and thus further

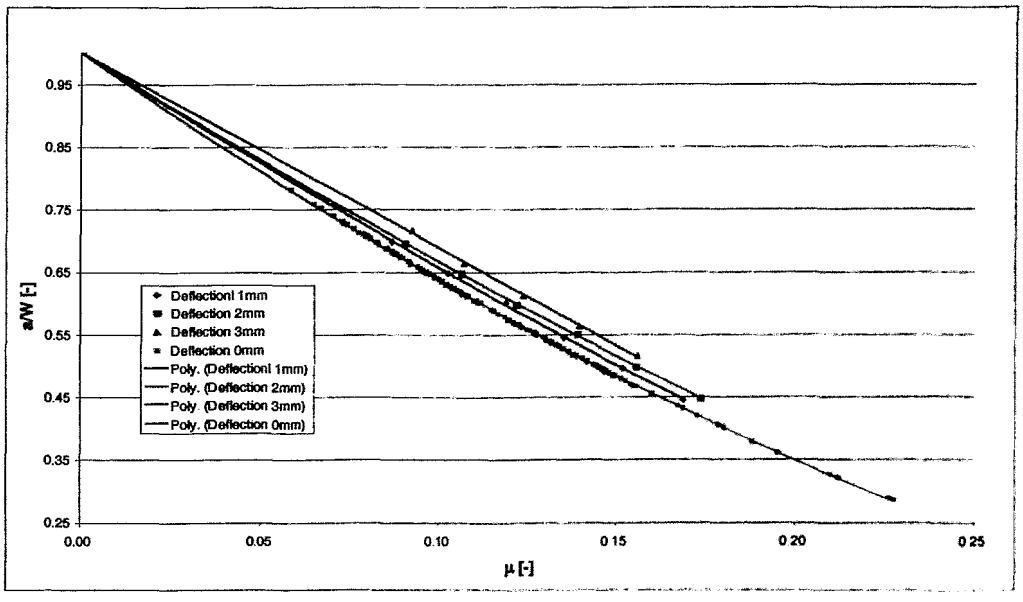

Fig. 11. Calibration functions curves determined from bent and eroded specimens

specimens were prepared.

Data for three different plastic deflections were obtained: 1, 2 and 3 mm. The results of the test are summarized in Fig. 11. Displayed data clearly show increasing movement of the curves with the deformation, but uneven trend prohibits

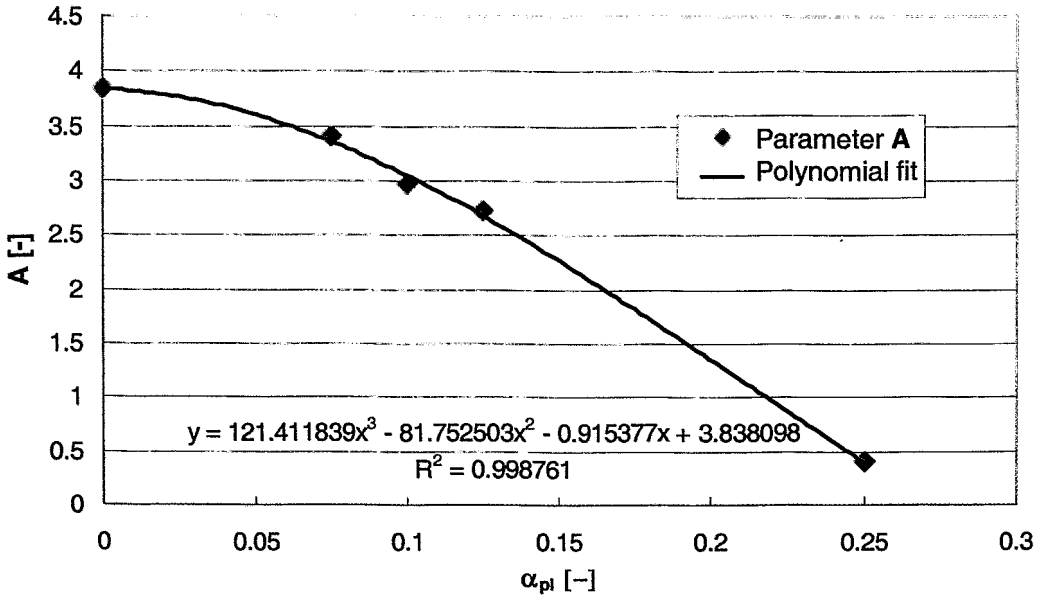

Fig. 12 Deflection dependence of correction function parameter A

quantification of the curves rotation and thus these data are not sufficient for the calibration curves deflection dependence evaluation.

The uneven trend of the curves shift with the deflection shows that data have scatter and thus large amount of data must be used in order to obtain reliable results. Complicated preparation of these specimen lead to the use of already tested standard specimens together with the bent + eroded specimens for the calibration curve movement evaluation. Data divided into groups according to their deflection, as described earlier, were further used together with data obtained with notched + eroded specimens.

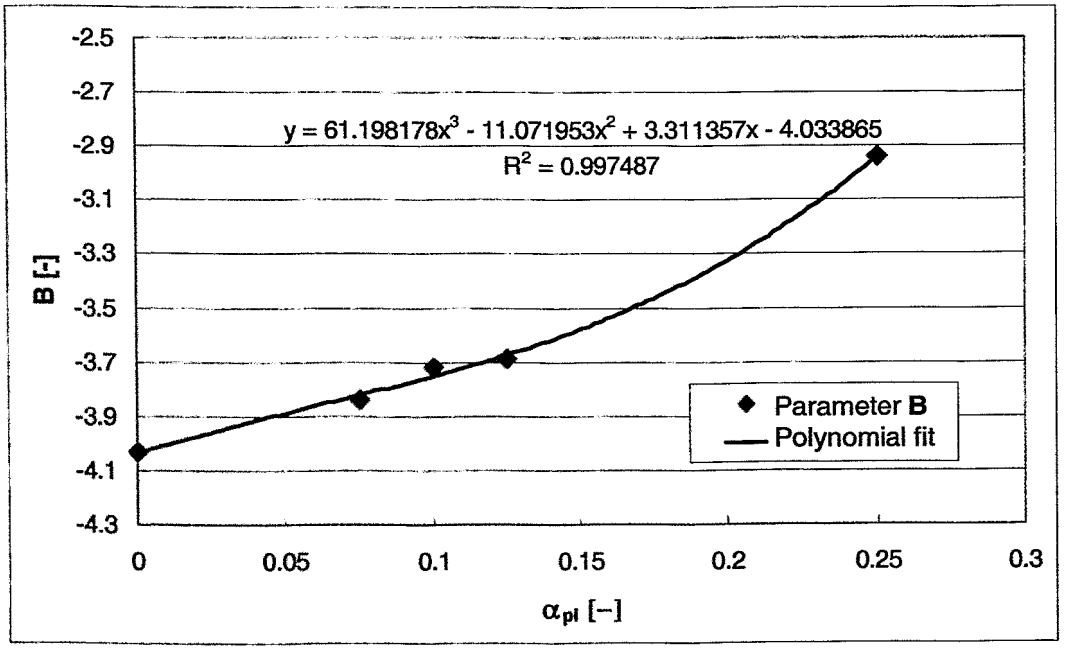

Fig. 13. Deflection dependence of correction function parameter B

Firstly, the polynomials of second degree according to Eq. 9 were fitted to the data for considered deflection levels. Parameters of the fit function were subsequently plotted in dependence on plastic angle, Figs. 12 and 13 and parameters ***A*** and ***B*** were expressed as a function of the plastic angle, Eqs. 10 and 11. In some cases the fit itself was following very well the data for particular deflection, but the fit parameters were not following common trend of the fit coefficients so these parameters were not used for the ***A*** and ***B*** deflection dependence fit.

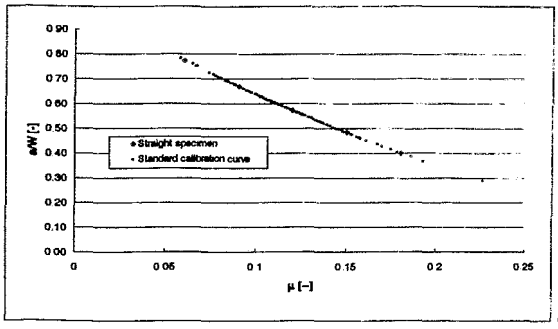

Fig.14. Fit for straight specimens

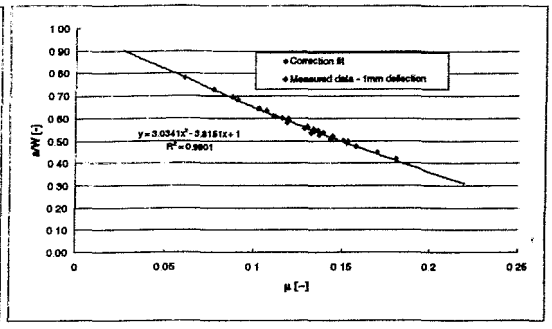

Fig.15. Fit to data with deflection 1mm

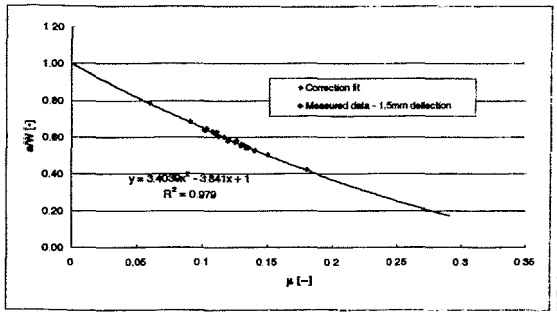

Fig.16. Fit to data with deflection 1.5mm

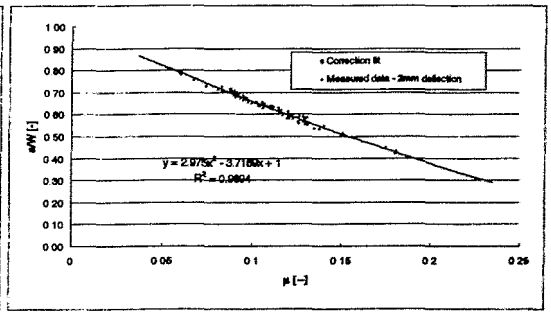

Fig.17. Fit to data with deflection 2mm

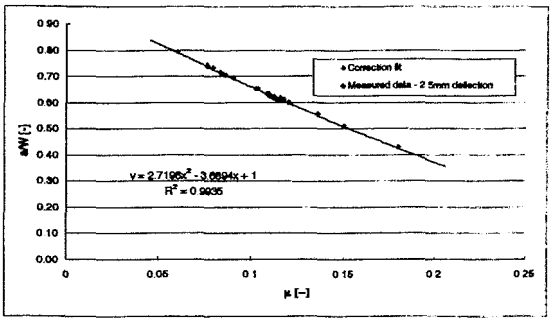

Fig.18. Fit to data with deflection 2.5mm

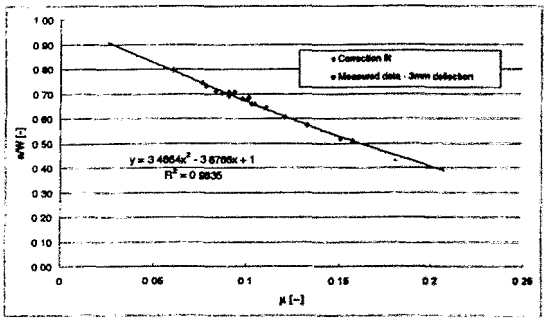

Fig.19. Fit to data with deflection 3mm

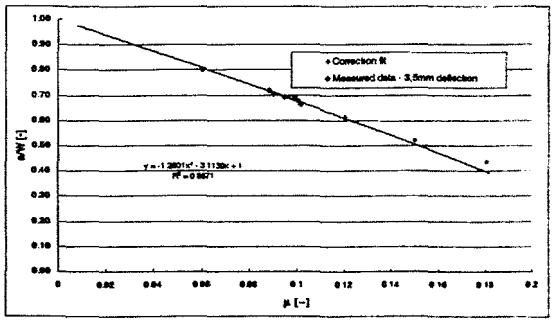

Fig.20. Fit to data with deflection 3.5mm

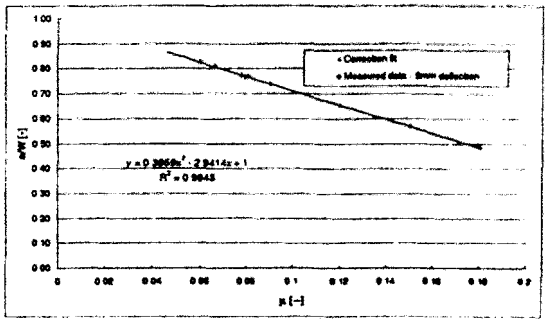

Fig.21. Fit to data with deflection 5mm

$$A = 121.4118 \bullet \alpha_{pl}^{3} - 81.7525 \bullet \alpha_{pl}^{2} - 0.9154 \bullet \alpha_{pl} + 3.8381 \qquad (10)$$

$$B = 61.1982 \bullet \alpha_{pl}^{3} - 11.07\ 20 \bullet \alpha_{pl}^{2} + 3.3114 \bullet \alpha_{pl} - 4.0339 \qquad (11)$$

where $\alpha_{pl} = \frac{\Delta_{pl}}{S/2}$.

Reliability of the Eq. 9 with parameters defined by Eqs. 10 and 11 was checked on the collected database and very good agreement was found, Figs. 14-21.

Movement of proposed calibration curves with deflection can be seen in Fig. 22.

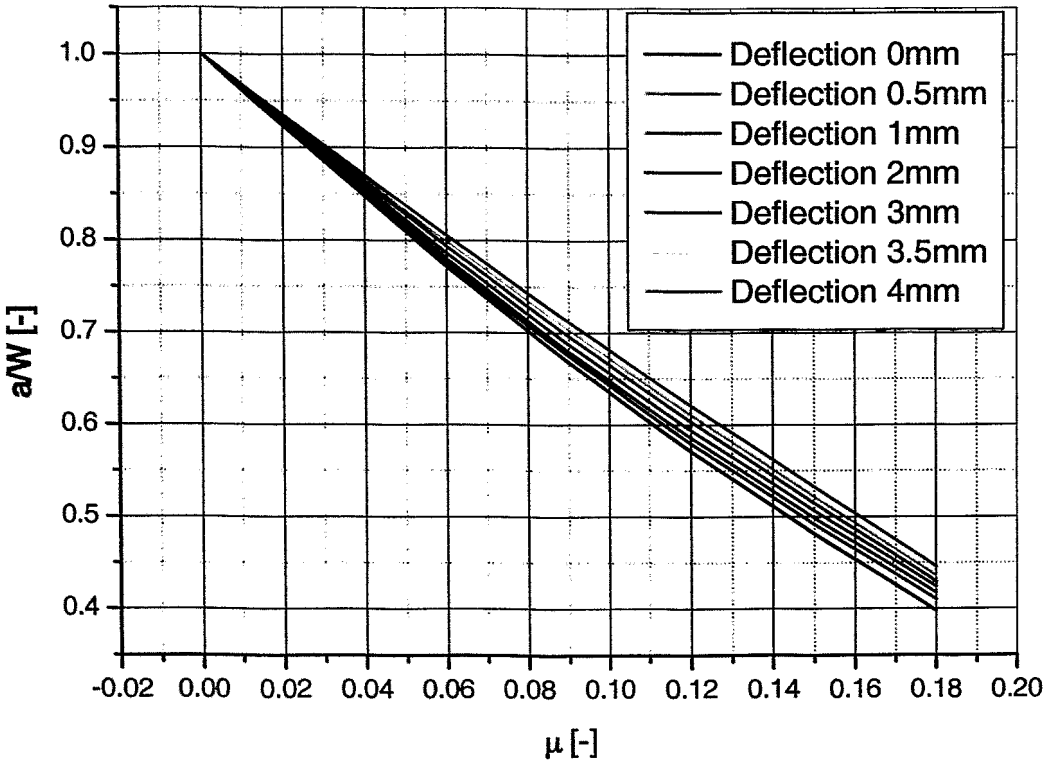

Fig. 22. Corrected calibration curves independence on the specimen deformation

6 Application of correction functions

The newly proposed correction function performance was checked on available experimental data together with previously published correction methods discussed in Chapter 3. For the correction assessment the elastic modulus obtained from tensile tests was used without any additional adjustments. The accuracy of the final crack length was observed instead of Δa, because in the Δa calculation the error of the a_0 measurement is included. The same accuracy limits according to ASTM 1820 as for the crack extension were applied for the data validation. The comparison of the results obtained without any correction, with newly proposed correction and with the other two corrections can be seen in Fig. 23. There is clearly visible increasing trend of the error with increasing deflection in cases of uncorrected data and data corrected

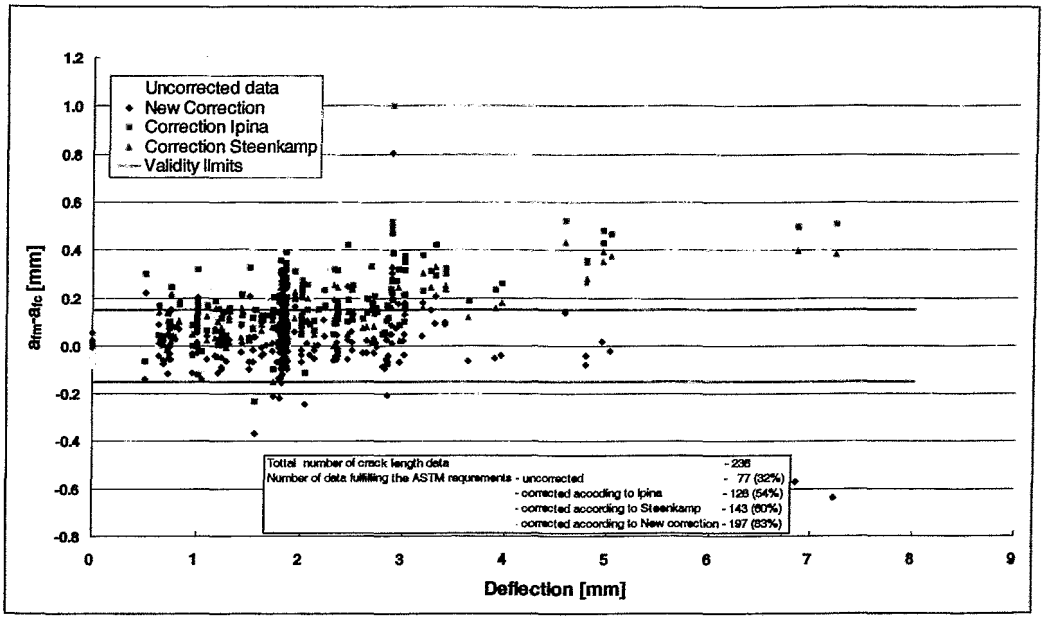

Fig. 23. Comparison of uncorrected and the values corrected according to Steenkamp, Ipiña and the new procedure

according to Steenkamp or Ipiña. The trend of all these curves is the same, but the slope is different. The best results out of these can be obtained with Steenkamp's correction, but still many data are out of the validity limits. The new correction function provides data with almost horizontal trend and data evenly distributed around 0 axis. This trend was attained up to deflection 5mm, data at deflection 7mm exhibit over corrected-values.

Example of J-R curve evaluated with the use of the new procedure is depicted in Fig. 24.

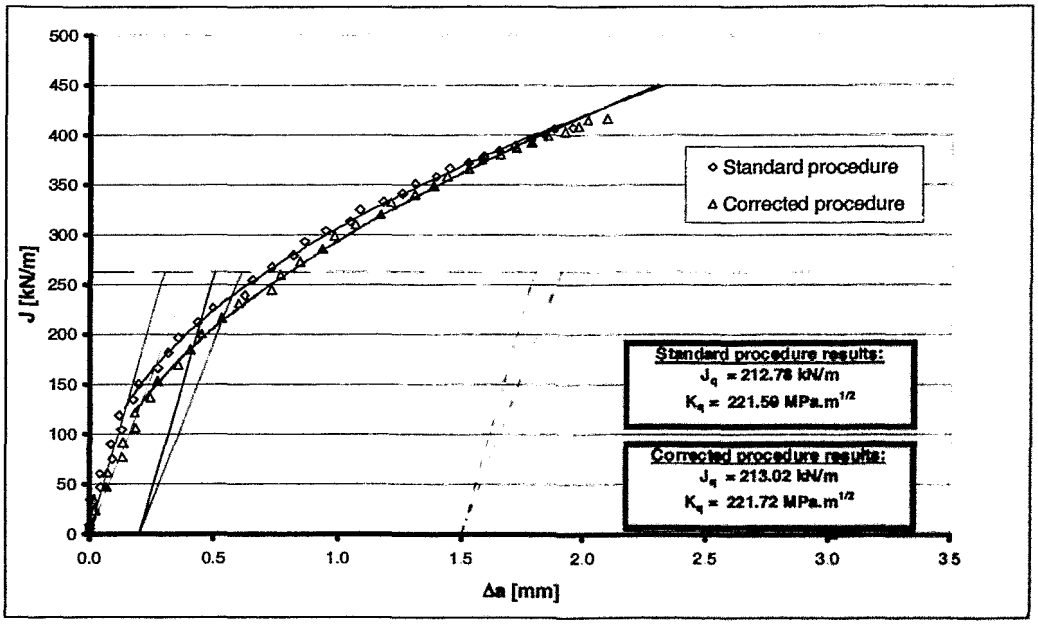

Fig. 24. Example of corrected J-R curve according to proposed correction function Δ_{pl}=1.82 mm, α=0.091, a_{fm}= 7.16mm, uncorrected a_f= 6.97mm, corrected a_{fc}= 7.13mm

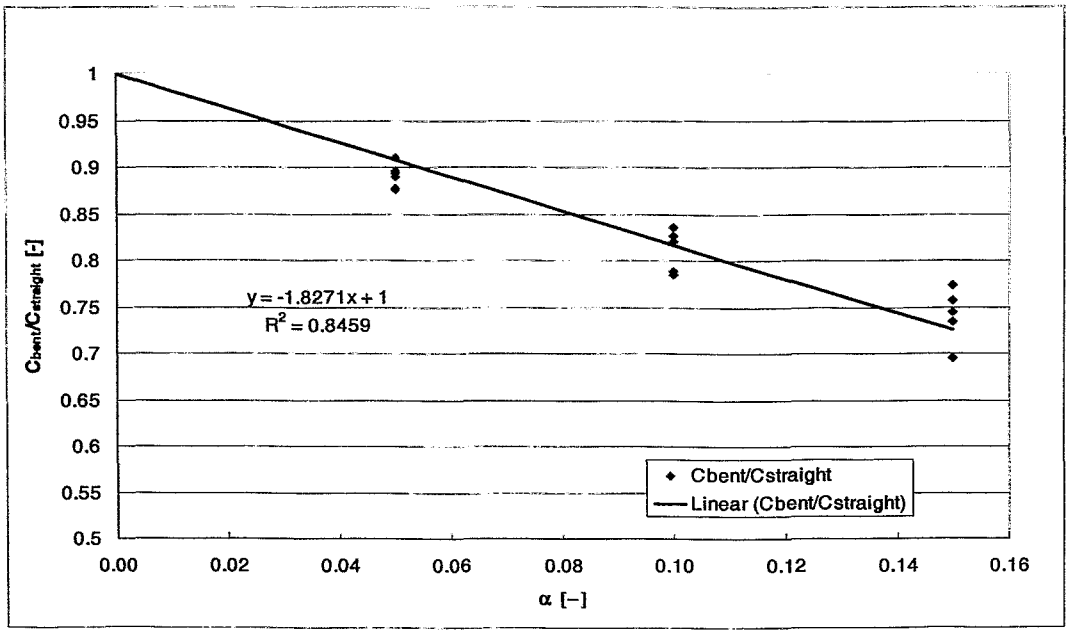

Fig. 25. Determination of Steenkamp's correction coefficient for Charpy size specimen

Ipiña's correction is based on the geometrical changes and it should be independent of the specimen geometry. Its performance for Charpy size specimens is rather poor. A little bit better results were obtained with Steenkamp's deformation based correction. This correction was derived for 3point bent specimen of cross section 12.5mm x 25 mm. It seems that this experimentally validated correction is not size independent and thus the modification of the proportionality coefficient could provide better results. Steenkamp validated his FEM calculations by specimen bent up to certain level, then spark-eroded notch was introduced and the compliance of such a specimen was measured and compared with the straight one. On the basis of the ratio

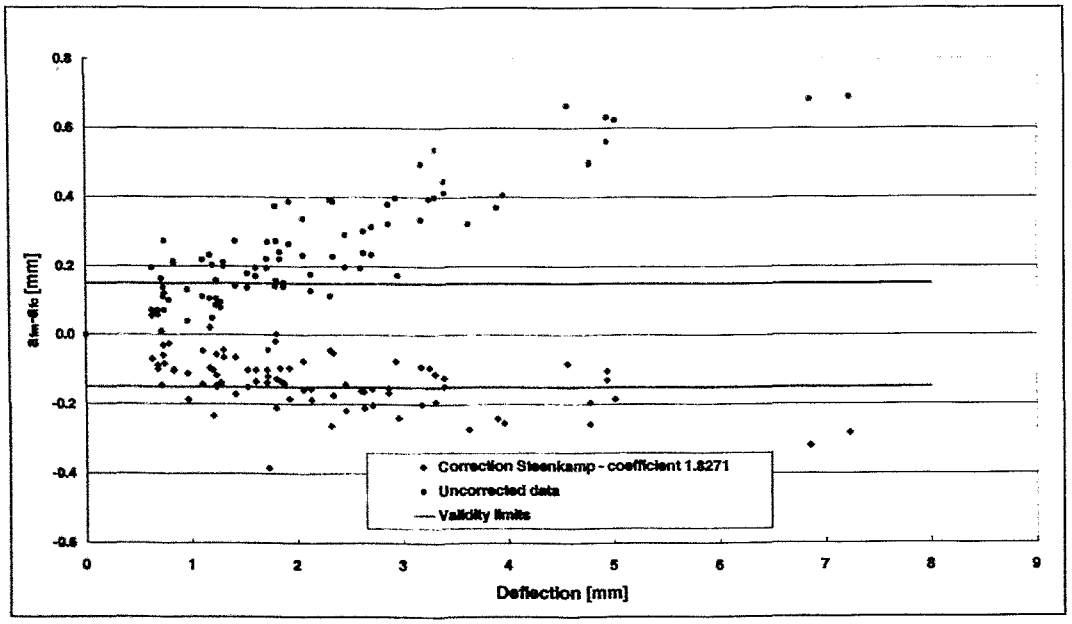

Fig. 26. Steenkamp's correction with the coefficient determined for Charpy size specimen

between bent and straight specimen compliance Steenkamp confirmed his calculations, Fig. 3. Within the present experimental program several specimens were prepared in similar way, so it enabled a possibility of direct determination of Steenkamp's correction function coefficient for Charpy size specimen, Fig. 25. With the use of determined correction function coefficient the measured values were corrected. Corrected data, Fig. 26, exhibit smaller scatter and lower error, but the data seem to be over-corrected and many data are out of validity limits. The correction coefficient obtained from measured data on Charpy size specimens over-corrects the compliances and provides longer crack lengths in comparison with measured ones.

From the previous results it can be inferred that the correction function could be size dependent, because previously tested methods of Steenkamp and Ipiña were working well according to the authors for the specimens with 12.5mm x 25 mm cross section. However for the Charpy size specimens the crack lengths were under-predicting as it was shown here. In order to evaluate the performance of the new correction function previously tested 12.5mm x 25mm size specimens were evaluated. For these specimens over-estimated crack lengths were obtained, so the newly proposed method is also not free of the size effect.

On the basis of analysis of the size effect results, the size effect was included into the new correction function and following form of the correction function is proposed:

$$A = 121.4118 \bullet \frac{B}{W} \bullet \alpha_{pl}^{\ 3} - 81.7525 \bullet \frac{B}{W} \bullet \alpha_{pl}^{\ 2} - 0.9154 \bullet \frac{B}{W} \bullet \alpha_{pl} + 3.8381 \qquad (12)$$

$$B = 61.1982 \bullet \frac{B}{W} \bullet \alpha_{pl}^{\ 3} - 11.07\ 20 \bullet \frac{B}{W} \bullet \alpha_{pl}^{\ 2} + 3.3114 \bullet \frac{B}{W} \bullet \alpha_{pl} - 4.0339 \qquad (13)$$

Movement of the calibration curves for Charpy size specimens and 12.5mmx25mm specimens, when coefficients A and B according to Eqs. 7 and 8 are used, can be observed in Fig. 27.

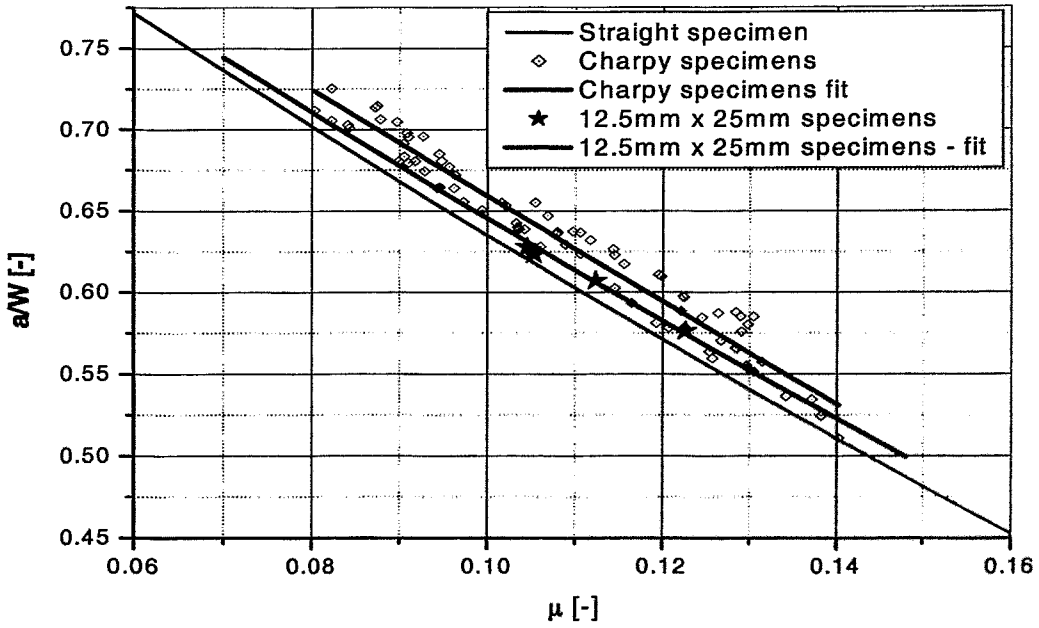

Fig. 27. Movement of the calibration curves in dependence on the specimen size at α_{pl}=0.1 for Charpy size specimens (Δ=2mm) and 12.5mmx25mm specimens (Δ=5mm)

The results for 12.5mm x 25 mm specimen obtained with use of the Eqs. 12 and 13 are summarized in Tab. 7. The agreement of measured and corrected crack lengths is very good, but limited amount of bigger specimens did not provide sufficient data for more serious verification of the proposed correction function including the size effect.

Tab. 7. Corrected results for 12.5mm x 25mm specimens

Specimen	Δ_{pl} [mm]	α_{pl} [-]	a_{0m} [mm]	a_{fm} [mm]	a_{0UC} [mm]	a_{fUC} [mm]	a_{fcorr} [mm]	a_{fm}-a_{fUC} [mm]	a_{fm}-a_{fcorr} [mm]
L34	5.18	0.10	12.84	15.18	12.84	14.87	15.18	0.31	0.00
L35	4.34	0.09	12.71	14.41	12.71	14.07	14.35	0.34	0.06
L37	4.85	0.10	13.45	15.58	13.45	15.47	15.70	0.11	-0.13
L38	4.87	0.10	13.53	15.70	13.53	15.52	15.80	0.18	-0.11

7 Discussion and summary

Developed correction function enables to attain results fulfilling the ASTM requirements for the crack length determination during J-R tests with the use of unloading compliance technique. The proposed correction function is experimentally based on measured and calculated crack lengths. It was derived with the use of Charpy size specimens made of steels.

The attention up to now was mainly focussed on the correction of the compliance value, considering it as a main factor assuming all the other calculations to be valid for bent specimens. In this study it was shown that the calibration function derived for a straight specimen is not independent of deflection, Figs. 8 and 9. With increasing specimen deformation the calibration curves change. The general shape of the function is the same, but it moves towards higher a/W values with advancing deformation. Analysis of measured data and formulas used for the crack lengths calculations led to assumption that the calibration curve is not translating, but rather moving around rotation point a/W=1 and μ=0. At this point there should be intersection of all curves if presumption of stiffness approaching zero for the specimen with through crack is valid. On this basis the new correction was developed, Eqs. 9, 10 and 11, and compared with other two corrections, Fig. 23. In comparison with these correction functions as published proved the newly proposed correction function superiority to the other methods, Fig. 23. The new function provided very good results up to a plastic deflections of 5mm, while Ipiña's and Steenkamp's formulas were clearly under-predicting the crack lengths from the beginning. However, Ipiña's and Steenkamp's methods were derived for bigger specimens, namely 12.5mm x 25mm cross-section. This means that possible influence of the size effect had to be investigated.

Ipiña's geometry change based correction is probably size independent, because it was developed from geometrical relations taking into account the specimens dimensions, so no further adjustments could be made. Insufficient performance of this method for the Charpy size specimens could be also caused by incorrectly chosen rotation factor. In the original work r_p=0.45 is used, but in literature also another values for the rotation factor could be found [9-7].

Conversely, Steenkamps function was based on FEM simulation of specimen with cross section 12.5mm x 25 mm. The correction function coefficient can be then related to considered geometry and then a new one for Chrapy size geometry could be

found. Using similar specimens preparation procedure during presented investigation, as Steenkamp used for verification of his function, it was possible to determine the coefficient for Charpy size specimens, Fig. 25. When this correction coefficient was used, over-corrected crack lengths were obtained, Fig. 26. Thus the experimentally based coefficient is not suitable for the investigated specimen size or considered correction function.

The size dependence of the proposed function was also observed on a few available specimens of the same cross section as used by the previous authors. In this case over-corrected crack lengths were obtained. On the basis of data analysis, correction function, Eqs. 12 and 13, taking into account deflection as well as size effect was proposed and verified on limited amount of larger specimens. This function already provided very good accuracy, Tab. 7. Though its applicability to larger specimens or generally specimens of different dimension has to be firstly proved on a larger data population than tested within the frame of the present investigation.

The results of the specimen size effect investigation, Fig. 27, give a hint that with decreasing B/W ratio of the specimens the deviation from the standard calibration curve decreases. Decreasing the ratio B/W by the factor of 2, the offset from the standard calibration curve is also approximately half of that for Charpy specimens. This gives a hint that if specimens with low B/W ratio are tested, relatively good agreement between measured and calculated crack lengths can be found with the use of the standard calibration curve. In the case when the specimens with higher B/W ratio (for example B/W=1) are tested, modified procedure for the crack length calculation with the use of the unloading compliance technique has to be applied in order to maintain the accuracy of the crack length determination.

Part of the presented research was also an investigation on the crack lengths evaluation with use of the averaging 9-point method. Method was compared with area based crack lengths and it was found that the method works very well for even cracks, but in case of more complex crack shapes too long cracks could be obtained, Tab. 4 and 5, Fig. 7.

8 Conclusions

In order to resolve the problems with the calculation of crack lengths using the unloading compliance technique a new method for the calculation was proposed. The new method based on experimentally obtained values of crack lengths and compliance measurements taking into account specimen deflection was derived. The new procedure provides very good agreement of measured and calculated final crack lengths. The method yields very good results up to plastic deflection of 5 mm for Charpy size specimens. Out of 238 measured final crack lengths 197 values fulfilled ASTM 1820 accuracy requirements while only 77 uncorrected values were acceptable.

The method presented here was developed on the basis of data collected for Charpy size specimens. The method was also tested on specimens of different size. Three point bend specimens with cross section 12.5mm x 25 mm were evaluated. Using the original form in which the function was proposed, over-corrected crack length values were obtained. When further modification was included, a function including specimen deformation and specimen size was proposed for the crack length calculation with the use of the unloading compliance technique. The modified function yields good results for both sizes of specimens. Reliability of the modified

function still has to be proved since only few specimens of larger dimensions were evaluated.

The results of the specimen size effect investigation hint that with decreasing B/W ratio of the specimens the deviation from the standard calibration curve for the straight specimen decreases. This fact stresses the necessity to use some modified procedure if the unloading compliance technique is used for testing of small size specimens like Charpy specimens in order to obtain reliable results.

9 References

1. ASTM E 1820-01. Standard Method for Measurement of Fracture Toughness. American Society for Testing and Materials, 2001.
2. ISO/DIS 12135. Metallic Unified method of test for the determination of quasi-static fracture toughness, Draft of International Standard ISO/TC 164/SC4, International Organisation for Standardisation, 1998.
3. Steenkamp, P.A.J.M.: J_R-Curve Testing of Three-Point Bend Specimen by the Unloading Compliance Method, Ph.D. thesis, Delft University of Technology, Netherlands, June 1985.
4. Steenkamp, P.A.J.M.: J_R-Curve Testing of Three-Point Bend Specimen by the Unloading Compliance Method, Fracture Mechanics 18th Symposium, ASTM STP 945, Philadelphia, 1988, pp. 583-610.
5. Ipiña, J., E, Santarelli, E., L.: Rotation corrections in three point single edge notch bend specimens, Journal of Testing and Evaluation, JTEVA, Vol. 17, No. 6, Nov.1989, pp. 381-393.
6. Džugan, J.: Unloading compliance for Charpy size three point bending specimens, FZR Arbeitsbericht FZR/FWSM – 02/2000, Jan. 2000.
7. Džugan J., Viehrig, H.W., Böehmert, J.: Unloading Compliance for Charpy Three Point Bending Specimens, National Conference with international participation Engineering Mechanics `2000`, Svratka, Czech Republic, May 2000, proc. pp. 19-24.
8. Schwalbe, K.-H, Neale, B.,K., Heerens, J.: The GKSS test procedure for determination the fracture behaviour of materials: EFAM GTP 94, GKSS procedure GKSS 94/E/60, October 1994.
9. Caminha, H.M., Bastian, F., L.: A study of relationship between rotational factors and COD values, Conference on Fracture Toughness Testing Methods, Interpretation and Application, London, UK, June 1982, pp. 72-102.
10. Wu, S.-X.: Plastic rotational factor and J-COD relationship of three point bend specimen, Engineering Fracture Mechanics, Vol. 18, No. 1, 1983, pp. 83-95.
11. Koledník, O.: An improved procedure for calculating COD in bend and CT specimens, Engineering Fracture Mechanics, Vol. 33, No. 5, 1989, pp. 813-826.
12. Wu, S.-X., Mai, Y.-W., Cottrell, B.: Plastic rotation factors of three-point bend and compact tension specimens, Journal of Testing and Evaluation, JTEVA, Vol. 16, No. 6, Nov. 1988, pp. 555-557.
13. Koledník, O.: Plastic overall rotational factors in bend and CT specimens, International Journal of Fracture39, 1989, pp. 269-286.